

# The new approach for dynamical regimes detection in geomagnetic time series

I S Knyazeva<sup>1,2</sup>, N G Makarenko<sup>1</sup>, Y A Kuperin<sup>2</sup> and L A Dmitrieva<sup>2</sup>

<sup>1</sup> Pulkovo observatory, Pulkovskoe sh. 65, Saint-Petersburg, Russia

<sup>2</sup> St. Petersburg State University, 7/9 Universitetskaya nab, St. Petersburg, Russia

E-mail: i.knyazeva@spbu.ru

**Abstract.** We suggest the new approach that could be used in the task of geomagnetic indexes forecasting. This approach based on the topological structure of the time series. The hourly data of different geomagnetic indexes were analyzed. We split the whole series to the calm parts, and geomagnetic storm preceding parts and find that the main measure of the topological structure of the series which called topological persistence differ significantly between these two groups.

## 1. Introduction

The task of magnetic storm forecasting remains an important problem of the space weather investigation. Approaches to storm forecasting depends on forecasting horizon. It could be divided by long-term (more than 7 days), medium-term (several hours to several days) and short term (several hours)[1]. The first two approaches based on forecasting of solar activity which lead to magnetic storm and the last one, short term forecast based on the information from spacecraft in the Sun-Earth libration point. Short term forecast is rather exact, but the alert time (less than 1 hour) is too short for practical use and the level of forecasting rate falls down rapidly with the growth of forecasting horizon.

It is widely accepted that the magnetic storm preceded by geoeffective pattern in solar wind speed and proton density and interplanetary magnetic field (IMF) parameters. It is known that for severe storm the IMF directed southward ( $B_z$  is negative) and the pressure is raised (solar wind speed and proton density raised). But this rule is not strictly [1]. G.Mansilla [2] and other authors shows absence of high linear correlation between the peak values of solar wind parameters with peak Dst index. This fact points to more complex geoeffective structure in solar wind parameters. The complex topological structure of time series could be described in terms of topological complexity. The topological data analysis is quite a new area in area such as data mining and computer vision. But its popularity growth rapidly. In this work we show one possible application for detection different dynamical regimes in geomagnetic time series.

## 2. Pre storm dynamics of solar wind and IMF

Building of geomagnetic storm prognosis on the base of geoeffective structures recognition is a fruitfull method (from Khabarova [1]). But the main problem in complexity of these structures. There are no strict conditions which always fulfilled before the storm started. It is known that for the most severe storm precede a strong increase of solar wind speed accompanied long-lasting negative  $B_z$  level, but for moderate storm these are not true. By the way, as shown



in papers [1] and [3] prediction of the moderate storm as an important task as strong storm forecasting. Moreover, phase shift (time) between geoeffective changes in solar wind parameters and interplanetary  $B_z$  changes from 0.5 to 5 hours, see [4]. Also, these structures differ during the solar cycle, because of difference physics properties of solar-interplanetary-magnetosphere coupling [5]. That's why it is hard to give a formal description of geoeffective conditions which must be performed before the storm, and consequently to make a good prediction system.

Below we provide a short intuitive introduction to an approach which allows to describe variations of some parameter during a specific time in several key features. This approach was borrowed from computational topology and now calls Topological Data Analysis (TDA).

### 2.1. Brief introduction to topological data analysis (TDA)

We would like to introduce the approach from computational topology which could describe the inner structure of time series. The full information about computational topology could be found in Edelsbrunner and Harer book [6]. Very clear introduction also could be found in [7]. To illustrate the main ideas, consider the graph of a continuous function  $f(x) \in \mathbb{R}$  and its sublevel set  $A_t = f^{-1}(-\infty, t)$ , i.e. points at which the function is below a specified level, see Figure 1. To study the topology of a function, one can measure how the topology of its sublevel sets evolves when the threshold is continuously and monotonically changing from lower levels to high. It is clear that for  $t_1 > t_2, A_{t_2} \subset A_{t_1}$ . Such a sequence of nested intervals is called filtration, precisely lower-star filtration. Sublevels consist of points and intervals in the horizontal axis. They are called the connected components, which splits the graph of its domain. Let consider the level 1.13 at Figure 1 and interval  $[a, b]$  consist from points  $f(x)$  which is below this level. Its boundaries  $\partial[a, b] = b - a$  can be combined with each other by sliding them along the interval. Formally, this means that they are topologically equivalent:  $a \cdot b : b = a + \partial[a, b]$ . The number of independent components for each level calls Betti number  $\beta_0$ . From figure 1 it could be seen that minimums of the function creates a connected component, and an adjacent maximum reduces the number of components. The level at which new component created calls birth of component, and level at which component was destroyed calls death of component. This fact is depicted in so called persistence diagram (see Figure 1, right. Here, on abscissa is the birth of all components, and on the ordinate - the level of death. Thus, at the minimum point (3.30, 0.76) new component appears, which collapses at adjacent maximum (1.40, 2.26). Corresponding to this event point (0.76, 2.26) is shown on the persistence diagram. In practice it is clear that small fluctuations in the graph correspond to points near the diagonal. Diagonal corresponds to a zero life expectancy. Long-lived or persistent components lies far from the diagonal. Stability Theorem states that for two functions that are close in terms of supremum metric corresponding persistence diagrams are also close.

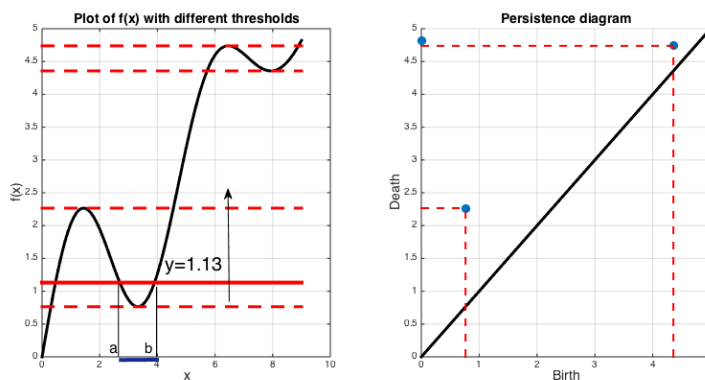


**Figure 1.** Example of lower-level set filtration of continuous function and corresponding persistent diagram

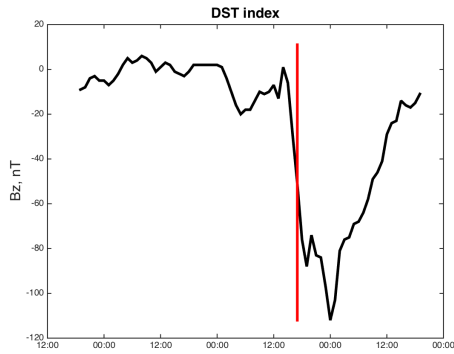


**Figure 2.** Dynamic of hourly Dst index. Vertical line indicates the beginning of the storm. We consider here that the point is a start of storm if the Dst index drops below  $-80$  nT and lasts under more than 3 hours.

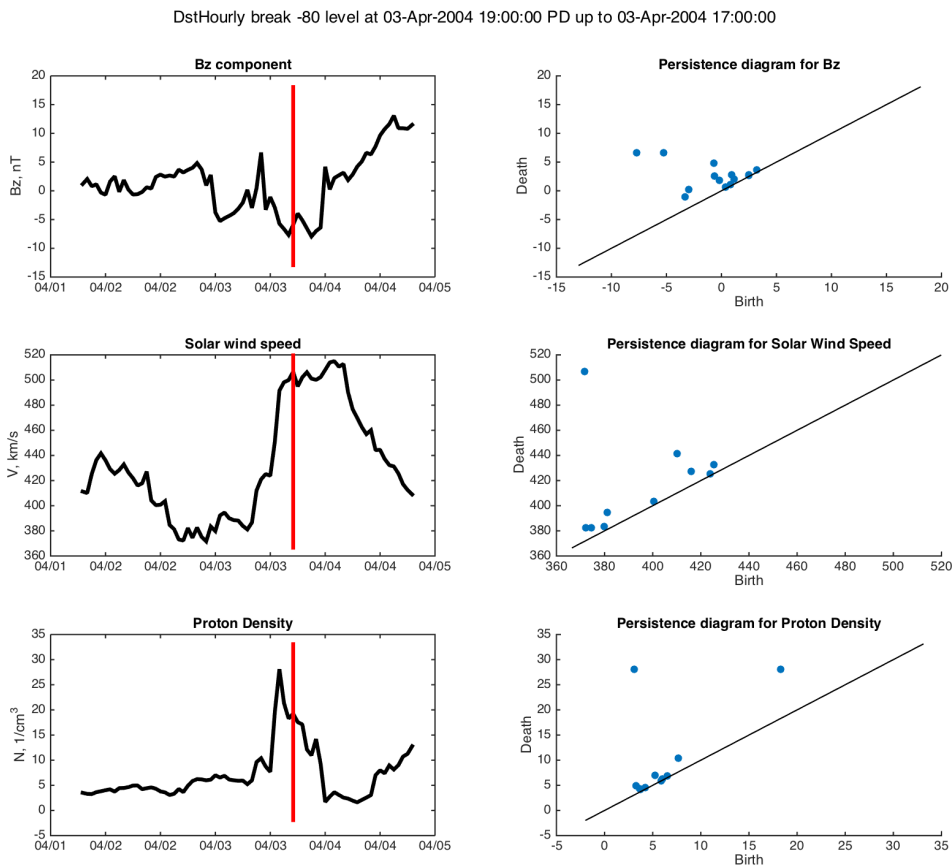


**Figure 3.** IMF  $B_z$  component, Solar wind speed and Solar proton density dynamic and pre-storm Persistence Diagram (PD). Vertical line indicates the start of the storm.

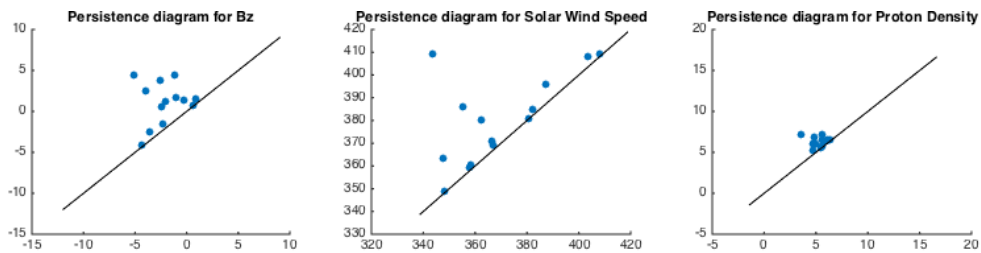


**Figure 4.** Persistence diagram of  $B_z$ , Solar wind speed and proton density for non storm case.

### 2.2. TDA of solar wind and IMF $B_z$ parameters

For solar wind speed, solar wind proton density and IMF  $B_z$  component hourly data were obtained from the website <http://www.srl.caltech.edu/ACE/ASC/level2/index.html>. Dst index data were downloaded from <http://spidr.ngdc.noaa.gov/spidr/>. At this work the period from 2001 to 2007 years was analysed. This period corresponds to solar maxima and declining phase of 23 Solar cycle. The solar wind and IMF data were processed as follows.

- The 48 hours period was taken up to 2 hours before the storm start for all three parameters. We consider here that the point is a start of strong storm if the Dst index drops below -80 nT and lasts below more than 3 hours and moderate storm if the Dst index drops below -50 nT and not exceed -100 nT during the whole storm phase.
- Persistence diagrams of solar wind speed, solar wind density and  $B_z$  component for this period were computed
- Separately were randomly chosen 100 fragments lasting 48 hours for each three parameters without storm during time fragments and after 24 hours from the end of the fragment.

At Figure 2 is shown an example of behaviour of the Dst index during the storm on 03 April, 2004. It could consider as a strong storm. The vertical line indicates the start of the storm. At Figure 3 corresponding series for solar wind speed, density and  $B_z$  component and persistence diagram is shown. We can see that for all three series, there are points at the diagrams which lie far from the diagonal, the location of these point describe the structure of the underlying series. For example, for  $B_z$  component appearance of negative movement could be seen as a separate two point in the left side of the diagram. The sharp increase in solar wind and proton density also could be seen as a separate long-living components. We find that for non-storm cases the picture of persistence diagram differs, typical view is shown at Figure 4.

### 3. Discussion and conclusion

In this work we represented new possible approach for pre-storm structure analysis. The persistence diagrams for pre-storm parts of time series of solar wind speed, proton density and  $B_z$  component were estimated. It turned up that persistence diagrams for pre-storm and calm periods differs significantly. That's mean that features from persistence diagram could be used in prediction systems, for example, such as described in the paper [8]

### Acknowledgments

This work was partly supported by RFBR grant # 15-01-09156

### References

- [1] Khabarova O V 2007 *Sun and Geosphere* **2**(1) 32-37
- [2] Mansila G A 2008 *Physica Scripta* **78**(4) 045902
- [3] Romanova N V, Pilipenko V A, Yagova N V and Belov A V 2005 *Cosmic Res* **43**(3) 186-193

- [4] Kane R P and Echer E 2007 *J. Atmos. Sol. Terr. Phys* **69** 1009-1020
- [5] Gonzalez W D, Tsurutani B T and Clua de Gonzalez A L 1999 *Space. Sci. Rev.* **88** 529-62
- [6] Edelsbrunner H and Harer J 2009 *Computational Topology, An Introduction* (AMS) p 241
- [7] Ghrist R *Elementary Applied Topology* ( ed. 1.0, Createspace) p 269
- [8] Shugai J S, Dolenko S A, Persiantsev I G and Orlov Y V 2006 *Pat. Recogn. and Im. Anal.* **16**(1) 79-81